(7) Semerak, S. N.; Frank, C. W. *Macromolecules* **1981**, *14*, 443.
(8) Gashgari, M. A.; Frank, C. W. *Macromolecules* **1981**, *14*, 1558.
(9) Holden, D. A.; Rendall, W. A.; Guillet, J. E. *Ann. N.Y. Acad. Sci.* **1981**, *366*, 11.
(10) van Aartsen, J. J.; Smolders, C. A. *Eur. Polym. J.* **1970**, *6*, 1105.
(11) Smolders, C. A.; van Aartsen, J. J.; Steinbergen, A. *Kolloid-Z. Z. Polym.* **1971**, *243*, 14.
(12) van Emmerik, P. T.; Smolders, C. A. *J. Polym. Sci., Part A-2* **1972**, *39*, 311.
(13) Feke, G. T.; Prins, W. *Macromolecules* **1974**, *7*, 527.
(14) Andreyeva, V. M.; Tager, A. A.; Tyukova, I. S.; Golenkova, L. F. *Polym. Sci. USSR (Engl. Transl.)* **1978**, *19*, 3005.
(15) Keuvahara, N.; Tachikawa, M.; Hamano, K.; Kenmochi, Y. *Phys. Rev. A* **1982**, *25*, 3449.
(16) van Aartsen, J. J. *Eur. Polym. J.* **1970**, *6*, 919.
(17) van Emmerik, P. T.; Smolders, C. A.; Geymeyer, W. *Eur. Polym. J.* **1973**, *9*, 309.
(18) Nojima, S.; Shiroshita, K.; Nose, T. *Polym. J.* **1982**, *14*, 289.
(19) Lauritzen, J. I.; Hoffman, J. D. *J. Res. Natl. Bur. Stand. Sect. A* **1960**, *64A*, 73.
(20) Cahn, J. W. *J. Chem. Phys.* **1965**, *42*, 118.
(21) Shultz, A. R.; Flory, P. J. *J. Am. Chem. Soc.* **1952**, *74*, 4760.
(22) Debye, P.; Coll, H.; Woermann, D. *J. Chem. Phys.* **1960**, *32*, 939.
(23) Debye, P.; Chu, B.; Woermann, D. *J. Chem. Phys.* **1962**, *36*, 1803.
(24) Scholte, Th. G. *J. Polym. Sci., Part A-2* **1971**, *9*, 1553.
(25) Kuwahara, N.; Nakata, M.; Kaneko, M. *Polymer* **1973**, *14*, 415.
(26) Nakata, M.; Kuwahara, N.; Kaneko, M. *J. Chem. Phys.* **1975**, *62*, 4278.
(27) Nakata, M.; Dobashi, T.; Kuwahara, N.; Kaneko, M.; Chu, B. *Phys. Rev. A* **1978**, *18*, 2683.
(28) Saeki, S.; Konno, S.; Kuwahara, N.; Nakata, M.; Kaneko, M. *Macromolecules* **1974**, *7*, 521.
(29) Dobashi, T.; Nakata, M.; Kaneko, M. *J. Chem. Phys.* **1980**, *72*, 6685.
(30) Shinozaki, K.; van Tan, T.; Saito, Y.; Nose, T. *Polymer* **1982**, *23*, 728.
(31) Chu, B.; Kubota, K. *Macromolecules* **1981**, *14*, 1837.
(32) Gelles, R.; Frank, C. W. *Macromolecules* **1982**, *15*, 1486.
(33) Fox, T. G., Jr.; Flory, P. J. *J. Appl. Phys.* **1950**, *21*, 581.
(34) Frank, C. W.; Gashgari, M. A. *Macromolecules* **1979**, *12*, 163.
(35) Torkelson, J. M.; Lipsky, S.; Tirrell, M.; Tirrell, D. A. *Macromolecules* **1983**, *16*, 326.
(36) Torkelson, J. M., unpublished results.
(37) Nishihara, T.; Kaneko, M. *Makromol. Chem.* **1969**, *124*, 84.
(38) Roots, J.; Nyström, B. *Eur. Polym. J.* **1979**, *15*, 1127.
(39) Blandamer, M. J.; Fox, M. F.; Powell, E.; Stafford, J. W. *Makromol. Chem.* **1969**, *124*, 222.
(40) Blackmore, W. R.; Alexander, W. *Can. J. Chem.* **1961**, *39*, 1888.
(41) Flory, P. J. "Principles of Polymer Chemistry"; Cornell University Press: Ithaca, NY, 1953; p 615.
(42) Billmeyer, F. W.; Stockmayer, W. H. *J. Polym. Sci.* **1950**, *5*, 121.
(43) Altares, T.; Wyman, D. P.; Allen, V. R. *J. Polym. Sci., Part A-1* **1966**, *2*, 4533.
(44) Cragg, L. H.; Dimitru, T. E.; Simkens, J. E. *J. Am. Chem. Soc.* **1952**, *74*, 1977.
(45) Brandrup, J.; Immergut, E. H., Eds. "Polymer Handbook"; Wiley: New York, 1975.
(46) Nierlich, M.; Cotton, J. P.; Farnoux, B. *J. Chem. Phys.* **1978**, *69*, 1379.
(47) de Gennes, P. G. "Scaling Concepts in Polymer Physics"; Cornell University Press: Ithaca, NY, 1979.
(48) Perzynski, R.; Adam, M.; Delsanti, M. *J. Phys. (Paris)* **1982**, *43*, 129.
(49) Sun, S.-T.; Izumi, N.; Swislow, G.; Tanaka, T. *J. Chem. Phys.* **1980**, *73*, 5971.
(50) Wieting, R. D.; Fayer, M. D.; Dlott, D. D. *J. Chem. Phys.* **1978**, *69*, 1996.
(51) Dlott, D. D.; Fayer, M. D.; Wieting, R. D. *J. Chem. Phys.* **1978**, *69*, 2752.
(52) Frank, C. W.; Gashgari, M. A. *Ann. N.Y. Acad. Sci.* **1981**, *366*, 387.
(53) Gelles, R.; Frank, C. W. *Macromolecules* **1982**, *15*, 741.
(54) Fitzgibbon, P. D.; Frank, C. W. *Macromolecules* **1982**, *15*, 733.
(55) Vala, M. T.; Haebig, J.; Rice, S. A. *J. Chem. Phys.* **1965**, *43*, 886.
(56) Ghiggino, K. P.; Wright, R. D.; Phillips, D. *J. Polym. Sci., Polym. Phys. Ed.* **1978**, *16*, 1499.
(57) Hirayama, F.; Lipsky, S. *J. Chem. Phys.* **1969**, *51*, 1939.
(58) Hirayama, F. *J. Chem. Phys.* **1965**, *42*, 3163.

Optical Properties of (Hydroxypropyl)cellulose Liquid Crystals. Cholesteric Pitch and Polymer Concentration

Rita S. Werbowyj and Derek G. Gray*

Pulp and Paper Research Institute of Canada and Department of Chemistry, McGill University, Montreal, Quebec, Canada H3A 2A7. *Received October 5, 1983*

ABSTRACT: Liquid crystalline solutions of (2-hydroxypropyl)cellulose (HPC) in water, acetic acid, and methanol were examined by optical microscopy, refractometry, optical rotatory dispersion, and optical diffraction. Light transmission through thin and thick layers of the liquid crystalline phase was measured spectrophotometrically. The apparent absorption of light by thick layers and the angular variation in reflected wavelength were in accord with a polydomain structure. The cholesteric pitch was determined as a function of HPC concentration from measurement of the reflection band wavelength and the average refractive index for short-pitch samples and by optical microscopy or laser diffraction for long-pitch samples. The reciprocal pitch varied as the third power of the HPC concentration. The data also followed the concentration dependence predicted in a recent theory (H. Kimura, M. Hosino, and H. Nakano, *J. Phys. Soc. Jpn.*, **51**, 1584 (1982)).

A large number of cellulose derivatives form lyotropic and thermotropic liquid crystalline phases.[1] The polymeric component of these phases consists of a linear chain of β-(1–4)-linked anhydroglucose units with a wide variety of *nonmesogenic* substituents on the hydroxyl groups. The cellulose backbone is optically active and cellulosic mesophases show cholesteric properties. Lyotropic systems often reflect visible light,[2,3] indicating that the cholesteric pitch is of the magnitude of the wavelength of light, but much larger pitch values ($P \sim 1$–10 μm) have been observed for some solutions of cellulose derivatives.[4,5] Cholesteric reflection has also been observed for solvent-free thermotropic cellulose derivatives at elevated[6] and room temperatures.[7]

In this paper, the relationships between the cholesteric pitch and some optical properties are summarized. The experimental variation in pitch with solvent concentration for (2-hydroxypropyl)cellulose (HPC) is presented. The results are compared with those for other cholesteric liquid crystalline materials and with theory.

Discussion of optical properties of cholesterics[8] is based on the theory of de Vries;[9] the interpretation of the fin-

0024-9297/84/2217-1512$01.50/0

gerprint texture of polymeric long-pitch cholesterics is based on the work of Robinson[10] and subsequent observations[11] on polypeptide systems.

Experimental Section

(Hydroxypropyl)cellulose samples HPC-E, HPC-L, and HPC-J were supplied by Hercules Inc. These samples, marketed under the trade names Klucel E, L, and J, respectively, were reported by the makers to have on average 3.6–3.8 hydroxypropyl substituents per anhydroglucose unit.[12] A slightly higher molar substitution for HPC-E has been reported recently in a careful ^{13}C NMR study by Lee and Perlin.[13] The molar mass of each sample was measured by short-column sedimentation equilibrium in water with a Beckman Model E analytical ultracentrifuge.[14] Solutions from 1.7 to 10.5 g/L were centrifuged at 12 000 rpm for 4 h. The values for molar mass calculated from an extrapolation to zero concentration were 60 000, 82 000, and 100 000 for HPC-E, HPC-L, and HPC-J, respectively. These values are in good agreement with the manufacturer's data and with a value of 73 000 measured by sedimentation velocity[15] for a dialyzed HPC-L sample. (The above molar masses are lower than values that we measured by low-angle laser light scattering in water, ethanol, and tetrahydrofuran, but difficulties were experienced with incomplete solution and time-dependent aggregation in the light scattering experiments.[14,16] This behavior has been observed for other cellulose derivatives.[17,18]) A sample of (acetoxypropyl)cellulose (APC) was prepared from HPC by esterification and characterized as described previously.[6]

Liquid crystalline solutions were prepared from HPC and water or organic solvents (AnalaR or spectral grades, as received). Aqueous samples were prepared by weighing dried polymer into 15-mL polyethylene-capped glass vials and adding known amounts of water. The capped samples were allowed to stand for at least 1 month. The concentration and uniformity of the liquid crystalline solutions that formed above 42% by weight HPC[16] were checked by gravimetric analyses of the mesophases. Aliquots of 10–20 mg of each HPC solution were transferred rapidly and carefully to preweighed aluminum differential scanning calorimeter pans. The weight was measured on a Cahn gram electrobalance. The water was removed by heating at 85 °C for 30 min and then at 105 °C to constant weight. Each analysis was performed in triplicate. The concentration in almost all cases was within 1% of the initially prepared composition. Organic mesophases were prepared and analyzed in a similar manner. This care was necessary because, as will be shown, the wavelength of light reflected from the cholesteric mesophases is very sensitive to the polymer concentration.

Optical rotatory dispersion (ORD) measurements were made with a Jasco ORD/UV5 spectropolarimeter. The ORD spectra of dilute isotropic solutions of HPC were measured in a standard 10-mL ORD sample cell at 21 °C. Aqueous D-glucose solutions were used as calibrants. The rotatory dispersion of the viscous and highly optically active liquid crystalline phase was measured on thin layers of mesophase sealed between two microscope slide cover glasses with epoxy resin. The thickness of the mesophase and cover glasses was measured with a precision micrometer. Some variation in thickness across the samples was evident, so for more precise measurements, the mesophase was sealed with wax in quartz cells with a 0.01-mm spacing (Hellma Canada). The cells were allowed to stand 24 h before they were mounted in the spectropolarimeter. This allowed the initial shear orientation of samples to relax and assume a more uniform texture. The samples were handled with care to avoid mechanical stress; slight pressure caused a striking effect on the optical properties. Measurements were made between 700 and 300 nm. Thin samples were necessary to keep the measured rotation within the ±2° range of the instrument. A sharp, intense reflection band was observed spectrophotometrically as an apparent absorption peak at the wavelength at which the sign of the optical rotation reversed. The absorption spectra were measured with a Cary Model 17 spectrophotometer; the near-infrared capability of this spectrophotometer allowed us to measure reflection bands to 1500 nm. The angular dependence of the reflection band wavelength was measured with a Pye Unicam SP8-150 spectrophotometer equipped with a variable-angle specular reflectance accessory. The mean refractive index of each mesophase sample was measured with an Abbé refractometer (Carl Zeiss Model 44159). Fingerprint line spacings were measured either by photographing the mesophase samples with a Reichert Zetopan microscope and Nikon F camera (with an etched scale slide as calibrant) or by photographing the diffraction ring produced when light from the helium–neon laser (Spectra-Physics 145) impinged at right angles on a sample of mesophase held between a dished microscope slide and cover glass.

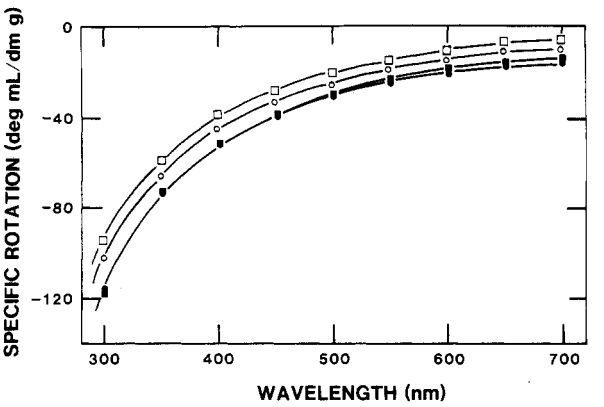

Figure 1. Optical rotatory dispersion for dilute solutions of (hydroxypropyl)cellulose in water (●), methanol (■), acetic acid (○), and Cellosolve (□) at 21 °C.

Results and Discussion

Dilute Solutions. The cholesteric properties of cellulose-based liquid crystals result from the presence in the anhydroglucose chain of asymmetric carbons which impart optical activity to cellulose and cellulose derivatives. The variation in optical rotation with wavelength for dilute solutions of (hydroxypropyl)cellulose in several solvents is shown in Figure 1. The curves show a monotonic increase in negative rotation with decreasing wavelength; the specific rotation varies approximately as the inverse square of the wavelength as expected for a plain negative optical rotatory dispersion (ORD) curve.[19] Molecules with chromophores in a chiral environment show anomalous ORD curves with an inversion of sign in optical rotation at the wavelength of absorption of intense chromophores and a peak in the corresponding circular dichroism (CD) spectra, where one component of circularly polarized light is preferentially absorbed by the chromophore.[19] (Hydroxypropyl)cellulose, like cellulose, has no chromophore in the visible or near-UV region of the spectra.

It is not yet clear how the chiral properties of the cellulose chain impart a cholesteric structure to the concentrated mesophase. It has been shown that an assemblage of long helical rods of a given handedness will produce a twisted nematic structure.[20–22] This model seems appropriate for helical polypeptide chains and there is strong evidence that the (hydroxypropyl)cellulose chains also assume a helical conformation in the solid state,[23] but whether a helical chain conformation is a necessary condition for formation of all cellulosic mesophases is still not known. The incorporation of an optically active solvent[24] or comonomer[25] in a stiff-chain mesophase is sufficient to generate the cholesteric structure, presumably without inducing a helical chain conformation, and cellulose itself exists in a planar zigzag conformation in the solid state.[26] Incorporation of cholesteryl ester side chains in a flexible silicone-based polymer also results in a cholesteric structure.[27]

Planar Texture of Cellulosic Cholesterics. Many cellulose-based polymers are observed to form anisotropic phases at polymer concentrations above about 35% polymer by weight.[1] Factors such as chain flexibility, molecular

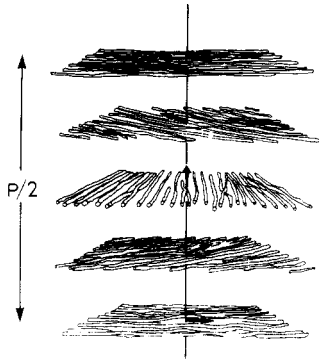

Figure 2. Sketch of a planar helicoidal, cholesteric arrangement made up of semiflexible chains. The helicoidal axis is vertical and the helicoidal pitch is P.

weight, and polymer–solvent interactions influence the critical concentration.[16,28-30] The persistence length of a chain molecule in the mesophase is assumed to be much greater than its contour length (although the direction of the chain elements may fluctuate about the preferred direction) and the chains tend to be parallel to each other. However, the presence of chiral elements causes the chains to be displaced a little from parallel. When the array of chains is constrained by a flat surface, the supermolecular helicoidal structure sketched in Figure 2 may in time develop. The "planar cholesteric" structure shows a very high optical activity when viewed along the helicoidal axis. The sign of the optical activity changes sharply at a wavelength, λ_0, which is a function of the temperature for thermotropic cholesterics and is also a function of concentration for lyotropic systems. Furthermore, when the sample is illuminated normally with white light, it reflects one circularly polarized component of light in a narrow wavelength band around λ_0. This reflection band if in the visible region of the spectrum gives rise to the intense iridescent colors characteristic of many cholesteric materials.

de Vries[9] developed a theory to account for the opical properties of planar cholesterics that is based on a model consisting of a large number of birefringent layers, each with its optical axis slightly displaced from its neighbors in a helicoidal arrangement. Variables in the theory are the helicoidal pitch, the layer birefringence, and the average refractive index of the material. According to this model, the wavelength λ_0 of normally reflected light in air is given by

$$\lambda_0 = \bar{n}P \tag{1}$$

where λ_0 is the wavelength of reflected light in air, $\bar{n}$ is the average refractive index of the mesophase, and P is the helicoidal pitch.

The rotatory power of the liquid crystal at wavelengths larger and smaller than that of the reflected light is given by

$$\theta = -\frac{\pi(\Delta n)^2 P}{4\lambda^2[1 - (\lambda/\lambda_0)^2]} \tag{2}$$

where θ is the optical rotation expressed in rad/nm at a wavelength λ and Δn is the layer birefringence.

The rotation induced by planar cholesterics shows an inversion of sign at λ_0, which resembles the Cotton effect for a chromophoric group in a chiral environment.[19] However, the physical basis of the effect is quite different and the magnitude of the rotation is much larger for planar cholesterics than for isotropic solutions of optically active components. This is illustrated in Figure 3, where the optical rotatory dispersion for thin layers of HPC mesophases is plotted in the same units as for the dilute solutions (Figure 1).

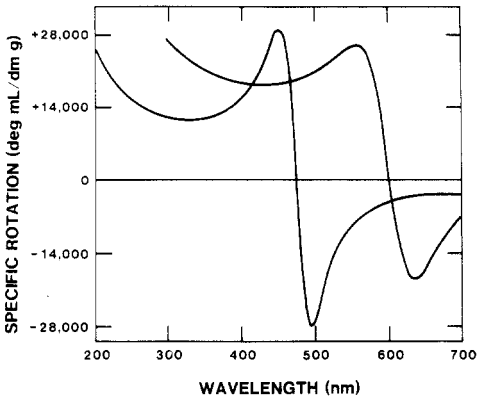

Figure 3. Examples of optical rotatory dispersion curves for planar texture (hydroxypropyl)cellulose mesophases. HPC-L sample in water (λ_0 = 475 nm) and methanol (λ_0 = 600 nm). Both samples 10 μm thick.

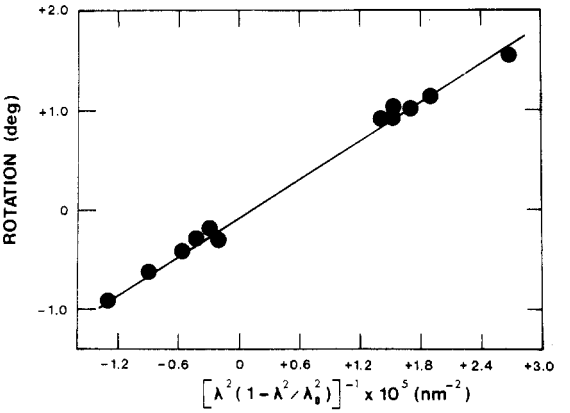

Figure 4. Optical rotation as a function of wavelength outside the reflection band for a planar aqueous HPC-J solution (thickness 69 μm, λ_0 = 524 nm, and $\bar{n}$ = 1.431). The value of Δn, measured from the slope, is 0.0075.

The positive rotation on the low-wavelength side of λ_0 shown in Figure 3 indicates that the helicoidal arrangement shown in Figure 2 is a right-handed structure.[9] The variation in rotation with wavelength given by eq 2 is observed for cellulosic cholesterics outside the reflection band region close to λ_0.[6] It is assumed that the average refractive index and the birefringence of the sample remain constant with wavelength. Plotting θ against the appropriate function of the wavelength from eq 2 gives a straight line (Figure 4), from whose slope a value for Δn, the layer birefringence, may be deduced. The magnitude of Δn governs the intensity and width of the cholesteric reflection band for very thin samples; Δn may independently be determined from the anisotropic refractive indices of the mesophase. The measurement and interpretation of the anisotropic refractive indices will be discussed in a subsequent paper.

Effect of Incident and Observation Angle on Reflected Wavelength. Light reflected from cholesteric materials shows a characteristic iridescence because, unlike normal absorption colors, the wavelength of the reflected light depends on the angle of viewing. A beam of incident light striking a planar structure (Figure 5a) at an angle ϕ (in air) is reflected at angle ϕ as an elliptically polarized beam of wavelength λ_0 (in air) given by[31]

$$\lambda_0 = \frac{\bar{n}P}{m} \sin \phi_B = \frac{\bar{n}P}{m} \cos \phi' \tag{3}$$

where ϕ_B is the Bragg angle between the incident beam

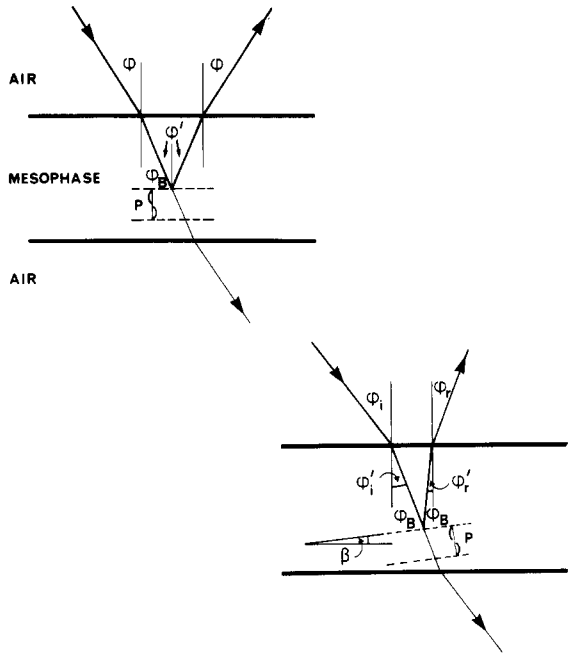

Figure 5. (a) Sketch of reflection and transmission for light incident at angle ϕ to planar cholesteric. (b) Sketch of reflection and transmission for light incident on a sample with planar cholesteric structure inclined at angle β to the plane of the sample. Broken lines indicate cholesteric structure with pitch P and axis normal to lines, ϕ_i and ϕ_r are the angles of incidence and reflection from the sample in air, and ϕ_B is the angle of incidence and reflection from cholesteric structures in the medium.

and a scattering plane in the mesophase and ϕ' is the angle of incidence and reflection inside the mesophase, which is related to the external angle ϕ by Snell's law

$$\phi' = \sin^{-1}(\sin \phi/\bar{n}) \tag{4}$$

and m is an integer. (For $\phi = 0$, only the first-order reflection, with $m = 1$, is found and the reflected light is circularly polarized.) The wavelength maximum for the reflection band as a function of incident angle can thus be found; a more detailed treatment[32] is necessary to predict the shape of the reflection band. Only light of wavelengths close to λ_0 is reflected; other wavelengths are transmitted so, for white incident light, the transmitted beam will show the complementary color to the reflected beam.

It is unusual to find extensive areas of a planar texture in cholesteric lyomesophases; examination between crossed polars often shows a grainy appearance characteristic of polydomain structure where the helicoidal axes are directed at all angles within the sample, rather than perpendicular to the sample walls. If ϕ_B is the Bragg angle between the incident light and a scattering plane in the mesophase that is oriented at an angle β to the sample surfaces (Figure 5b), then from eq 2 and Snell's law, Fergason[31] has shown that for samples with low birefringence, the wavelength of the component reflected at angle ϕ_r is related to the angle of incidence ϕ_i by

$$\lambda_0 = \frac{\bar{n}P}{m} \cos \frac{1}{2} \sin^{-1}\left(\frac{\sin \phi_i}{\bar{n}}\right) + \frac{1}{2} \sin^{-1}\left(\frac{\sin \phi_r}{\bar{n}}\right) \tag{5}$$

It is evident from Figure 5b that for a specified wavelength and angles of incidence and reflection, only those layers of mesophase with a single orientation angle, β, will contribute to the reflected light. For normal incidence and reflection, the color reflected from a polydomain texture is of course the same as for a planar texture. However,

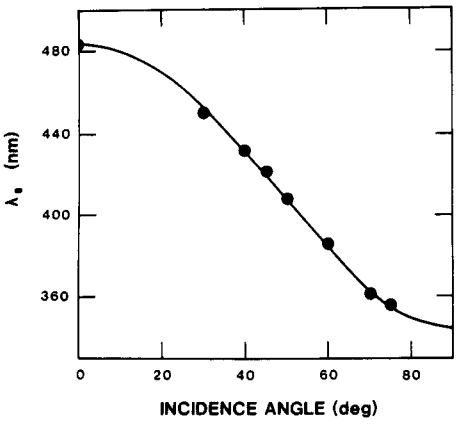

Figure 6. Angular variation in wavelength of reflected light for HPC-L, 64 wt % in water, measured with spectrophotometer and specular reflectance attachment (solid circles). The line is calculated from eq 5 with $\phi_i = \phi_r$ and experimental values for $\bar{n}$ and P of 1.436 and 336 nm, respectively.

transmission measurements on polydomain samples will also show absorption at wavelengths shorter than λ_0, rather than the sharp peak close to λ_0 shown by the planar texture. This is because the transmitted beam is diminished by light reflected at all angles from the randomly oriented planar structures.

Robinson determined the pitch values for solutions of poly(γ-ethyl L-glutamate) in ethyl acetate from measurements of the angular variation in wavelength of the scattered light.[33] This method has been applied to solutions of cellulose triacetate in trifluoroacetic acid.[34]

The angular variation in reflected wavelength for a (hydroxypropyl)cellulose–water mesophase was measured by means of a spectrophotometer with a specular reflectance accessory. The angles of incidence and reflection were equal for the experimental geometry. The variation in the wavelength of peak reflection with angle was in good agreement with that predicted by eq 5. Results are shown in Figure 6. The color of this sample thus changed from green when viewed normally to violet when viewed at lower angles.

Transmission through Thick Samples. For $\beta = 0$, normally incident light transmitted by the sample is depleted at $\lambda_0 = \bar{n}P$ by light reflected from the sample. For finite values of β, the transmitted light is depleted at shorter wavelengths. Thus for a sufficiently thick polydomain (nonplanar) sample, wehre the helicoidal axes are not oriented by wall or external field effects, all values of β are encountered as the light traverses the sample, and depletion will be observed for all λ less than or equal to $\bar{n}P$. Thus, in addition to losses to the transmitted beam from scattering from the birefringent fluid, reflectance from the randomly oriented cholesteric structures causes an apparent absorption for *all* wavelengths shorter than $\bar{n}P$.

The apparent spectrophotometric absorbance for a series of solutions of APC in acetone is shown in Figure 7. The absorbance of the solutions in 12-mm-diameter glass sample vials was measured in a double-beam instrument with a 50.0 wt % isotropic solution in the reference beam. Curve 3 of Figure 7 shows several distant features. This sample, which reflected a red color in white light, shows an increasing apparent absorbance with decreasing wavelength from 850 to about 720 nm. This is presumably due to scattering of light from the turbid birefringent fluid. The absorbance increases steeply in the 720–630-nm range, due to reflection from cholesteric structures with helicoidal axes approximately parallel to the beam directions.

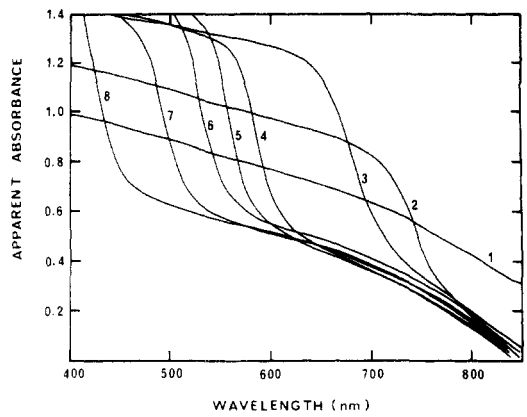

Figure 7. Apparent absorbance for thick (12-mm diameter) samples of (acetoxypropyl)cellulose in acetone. Concentrations in weight percent polymer: (1) 74.0; (2) 80.0; (3) 82.0; (4) 83.9; (5) 85.0; (6) 85.9; (7) 87.7; (8) 90.0.

However, the transmitted intensity does not drop again at higher wavelengths to give the apparent absorption peaks observed for thin samples but remains on a plateau, presumably because of reflections from cholesteric structures with axes at finite angles to the beam direction. As expected from the behavior of thin samples, increasing the concentration of polymer moves the steeply increasing portion of the absorption curves to shorter wavelengths (curves 4–8). The intensity of the apparent absorption seems to be somewhat greater for the higher concentrations. Curve 2 resembles curves 3–8, but the steep increase in apparent absorption is moving into the near-infrared region. A still lower concentration of polymer gives curve 1, which shows no steep portion because the reflection band is now at a wavelength beyond the range of the spectrophotometer. Solutions containing less than 30% APC are isotropic and show no significant absorption in this wavelength range. Solutions of cellulose triacetate in trifluoroacetic acid gave somewhat similar spectrophotometric results, but over a much more restricted wavelength range.[34] Thus the spectrophotometric method can give an indication of the cholesteric pitch of polymeric liquid crystals. However, a quantitative theory to account for the shape of the apparent absorption curves for thick turbid samples with multiple reflection is not yet available, and more precise results for λ_0 are available from ORD, CD, or spectrophotometric measurements on thin samples. Spectrophotometric results for thin layers of APC in acetone were reported previously.[6]

Long-Pitch Cholesteric Samples. The iridescent colors reflected from cholesteric liquid crystals with pitch values of the order of visible light are accounted for by de Vries' theory for planar cholesterics. However, the first reported polymeric mesophases (poly(γ-benzyl glutamate) in dioxane or methylene chloride) showed cholesteric structures with much larger pitch values. The structure of these liquid crystalline phases, which show a characteristic fingerprint-like pattern under the microscope, was first elucidated by Robinson.[10] He deduced that the pattern resulted from viewing a cholesteric structure at right angles to the cholesteric axis; the spacing of the alternating light and dark lines corresponded to half the pitch of the supermolecular helicoidal arrangement. Robinson noted the correspondence between a sample of mesophase showing this fingerprint texture and a diffraction grating. For a grating with a spacing of $P/2$ (Figure 8a), the diffraction condition in the medium is

$$\lambda_0 = \frac{\bar{n}P}{2m}(\sin \phi_i' + \sin \phi_r') \qquad (6)$$

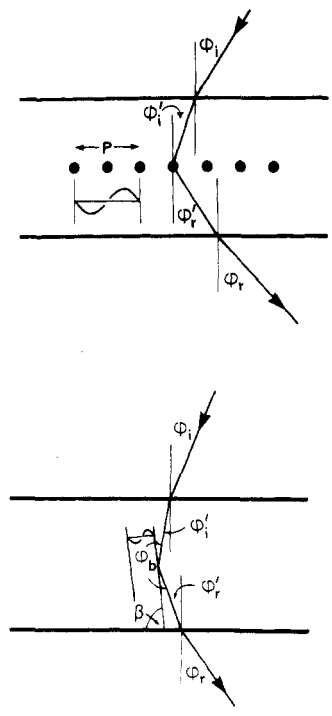

Figure 8. (a) Sketch for diffraction from a long-pitch cholesteric structure with helicoidal axis parallel to the surfaces of the samples. The distance $P/2$ between the dots represents the periodicity in refractive index of the fluid. (b) Alternative reflection model for scattering from long-pitch cholesteric structure. Compare with Figure 5b.

where λ_0 is the incident wavelength in air, $\bar{n}$ is the refractive index of the medium, and m is an integer. Neglecting again the difference in refractive index between glass and liquid crystalline medium, the beam directions in air and in the mesophase are related by Snell's law (eq 4), and eq 6 becomes

$$\lambda_0 = \frac{P}{2m}(\sin \phi_i + \sin \phi_r) \qquad (7)$$

This equation holds for a grating of periodicity $P/2$ for reflection and transmission, as well as for a grating covered by a medium of any refractive index whose surfaces are parallel to the mean grating surface.[35] (There is some confusion between diffraction and Bragg scattering conditions in the literature on fingerprint patterns.) For normal incidence where $\phi_i = 0$, eq 7 reduces to the equation employed by Robinson.[10] It is of course a simplification to regard the fingerprint texture as a two-dimensional phase grating; the lines actually correspond to *planes* of continuously varying refractive index oriented normally to the glass surfaces. Nevertheless the line spacings observed by light microscopy are very regular, leading to grating-like behavior. This has been observed in many concentrated polypeptide solutions[10,11] and has also been observed for solutions of some cellulose derivatives[5,36,37] and for the polysaccharide schizophyllan in water.[38] Fingerprint patterns randomly oriented in the plane of the sample when illuminated normally with monochromatic light produce a diffraction ring on a screen placed behind the sample and perpendicular to the beam. Although higher diffraction rings have been reported for polypeptide solutions,[10] only a single ring has been observed for polysaccharides[38] and cellulose derivatives.

An alternative to the diffraction approach is to consider Bragg-like reflection from those cholesteric planes in a polydomain structure which are oriented almost perpendicularly to the glass plates (Figure 8b). In this case, it

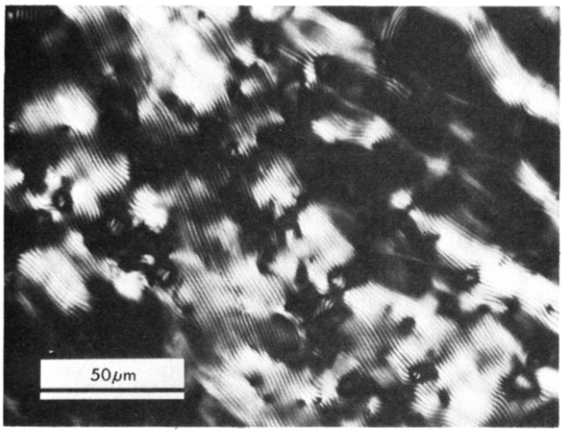

Figure 9. Fingerprint lines for 43 wt % HPC-L solution in acetic acid.

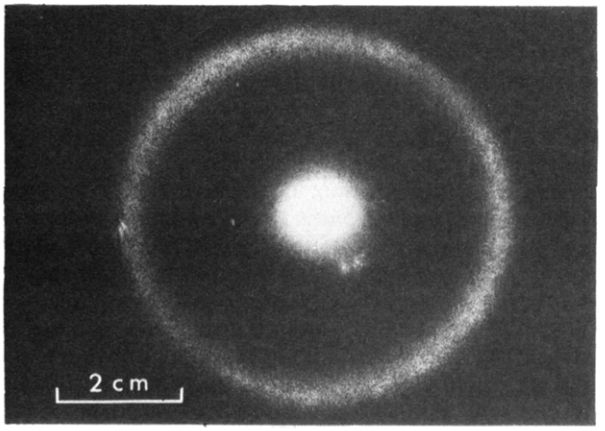

Figure 10. Light diffraction pattern for ~39 wt % HPC-L solution in acetic acid with a He–Ne laser light source. Sample-to-film distance was 6.6 cm.

can be readily shown by analogy with Fergason's method that the wavelength of the light passing through the sample and emerging at angle ϕ_r is related to the angle of incidence ϕ_i by

$$\lambda_0 = \frac{\bar{n}P}{m} \sin\left[\frac{1}{2}\sin^{-1}\left(\frac{\sin\phi_i}{\bar{n}}\right) + \frac{1}{2}\sin^{-1}\left(\frac{\sin\phi_r}{n}\right)\right] \tag{8}$$

For normal incidence ($\phi_i = 0$), this equation is equivalent to the refraction-corrected Bragg scattering condition for a fingerprint pattern given by Van, Norisuye, and Teramoto.[38] These authors also describe a simple method to account for the thickness of the sample and for refraction at the glass surfaces enclosing the sample.[38] For small values of ϕ, where $\phi \sim \sin\phi$, eq 8 reduces to eq 7.

Cellulose derivatives show long-pitch cholesteric structures in solvents that allow mesophase formation at relatively low volume fractions of polymer. A typical fingerprint pattern is shown in Figure 9. The fingerprint line spacings decrease with increasing polymer concentration until they are no longer resolvable in the optical microscope. Figure 10 shows an example of the diffraction ring produced by a HPC-L–acetic acid mesophase illuminated normally with a helium–neon laser. The diffraction rings are rather broad, leading to some uncertainty in the pitch values. Figure 11 shows the variation in pitch with concentration for HPC-L in acetic acid. (The pitch values calculated from the radius of the diffraction ring and eq 7 differ slightly from the microscopically observed pitch values because of sample and glass thickness and distortion

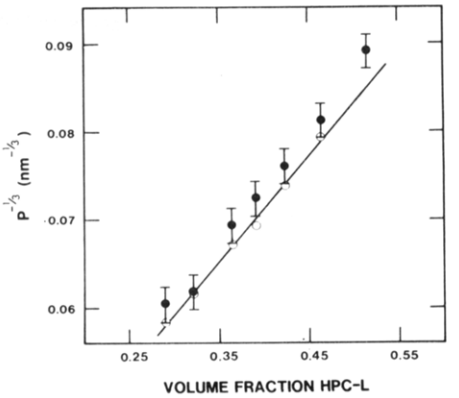

Figure 11. Variation in helicoidal pitch with volume fraction of HPC-L in acetic acid. Open circles from light microscopy. Closed circles with error bars from laser diffraction measurements (see text).

caused by the curved surface of the dished microscope slides used to hold the samples.)

The colors resulting from cholesteric reflection (eq 5) and from the diffraction grating effect (eq 7) are readily distinguished. Cholesteric colors are best viewed in reflection against a black background and the wavelength varies only slight with the viewing angle. The diffraction colors from cholesteric samples with values of P larger than the wavelength of visible light are most readily observed with sample between light source and viewer, and the colors are very sensitive to viewing angle. The dependence of wavelength on viewing angle may be calculated from eq 5, 7, and 8. For example, with $\phi_i = 0$, $\bar{n} = 1.4$, and $m = 1$, cholesteric reflection from a sample with a pitch of 400 nm ranges from a peak wavelength of 560 nm when viewed normally ($\phi_r = 0$) to 529 nm when viewed at $\phi_r = 60°$. However, the wavelength of the first-order diffraction color from a sample with a pitch of 2000 nm increases across the visible spectrum from 400 to 700 nm as the angle of viewing increases from $\phi_r = 23°$ to $\phi_r = 42°$. In contrast to the reflection colors (Figure 6), the diffraction colors were too faint to measure accurately with the spectrophotometer and reflectance attachment but the variation in color with angle was observed qualitatively.

Cholesteric Pitch and Polymer Concentration. In his pioneering study of polypeptide liquid crystalline solutions, Robinson[10] observed that the pitch of the helicoidal structure varied inversely as the square of the polymer concentration

$$1/P \propto \phi^2 \tag{9}$$

where ϕ is the volume fraction of polymer Subsequent work by Robinson[11] and others[33,39] has shown that the magnitude of the pitch and even the sense of the helicoidal arrangement for a given polypeptide may be a function of solvent, temperature, and molecular weight and that these factors affect the relationship between pitch and polypeptide concentration. In general, experimental results for single-stranded polypeptides may be fitted to the relationship

$$1/P \propto \phi^x \tag{10}$$

where x has a value between 1 and 2.[39] Iizuka found x to be 1.1 for double- and triple-stranded polyribonucleotide liquid crystals.[40]

Cellulose-based liquid crystals display a somewhat steeper inverse dependence of pitch on concentration. Values of x equal to 3 have been reported for (hydroxypropyl)cellulose in water[41] and (acetoxypropyl)cellulose in

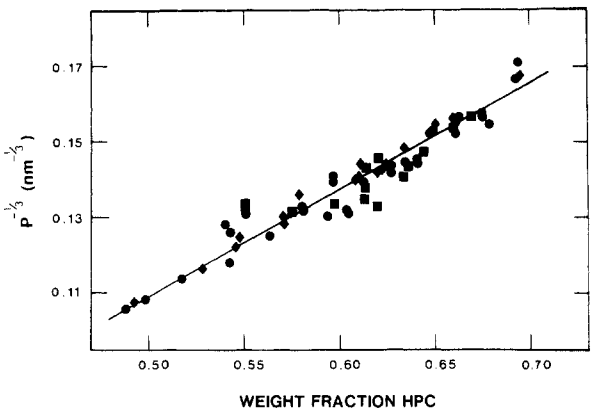

Figure 12. Variation in helicoidal pitch, P, with weight fraction of HPC-E (♦), HPC-L (●), and HPC-J (■) in aqueous solution. Values of P derived from ORD or spectrophotometric data.

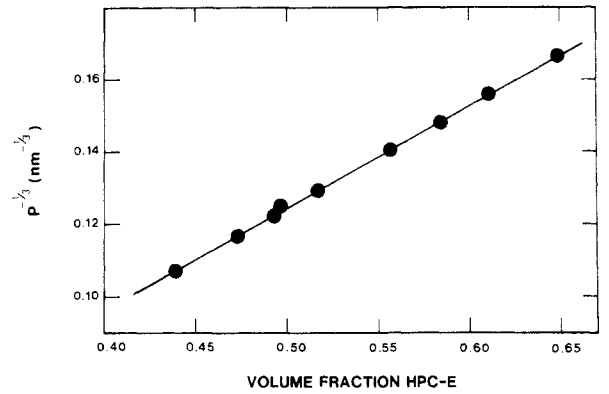

Figure 13. Helicoidal pitch, P, measured spectrophotometrically as a function of HPC-E volume fraction in water.

acetone.[6] Further data on (hydroxypropyl)cellulose are presented here. Long-pitch samples of HPC in acetic acid display fingerprint lines whose spacings follow the inverse third power relationship with volume fraction (Figure 11). Samples were reflection bands in the visible range also follow this relationship. Figure 12 shows data for several HPC samples in water. In this case, the concentration is given as the weight fraction of polymer in water. The reflection band wavelength, λ_0, was found from ORD or spectrophotometric measurements and the mean mesophase refractive index at the concentration in question was measured with an Abbé refractometer. The scatter in the points is not surprising in view of the different samples and methods used. Figure 13 shows spectrophotometric results for aqueous solutions of HPC-E; these results are more precise. However, care must be exercised in assigning any functional dependence of pitch to concentration because of the relatively small changes in concentration involved. (Replotting the data from Figure 13 as $P^{-1/2}$ against volume fraction still gives a plausible straight line but with a slightly lower correlation coefficient.) To avoid ambiguity, measurements are required over as large a concentration range as possible.

To achieve this, we sought a single polymer–solvent system that would give cholesteric mesophases with pitch values ranging from those measurable in an optical microscope (fingerprint patterns) to those of the magnitude of the wavelength of visible light (reflection colors). (Hydroxypropyl)cellulose in acetic acid gave both long-pitch samples and cholesteric colors but, at the high concentrations needed to form colors, the material was stiff and difficult to handle. However, the same polymer in methanol gave the required results, with pitch values

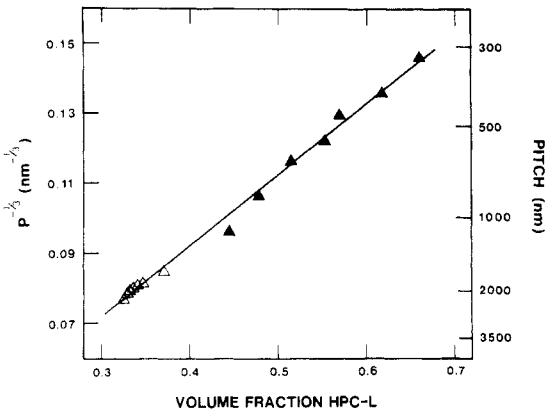

Figure 14. Plot of $P^{-1/3}$ against volume fraction of HPC-L in methanol. Open triangles are results for long-pitch samples measured by optical microscopy or laser diffraction. Closed triangles are from reflection wavelengths measured by ORD or spectrophotometrically.

ranging from 300 to over 2000 nm as the concentration of polymer decreased. Again, a reasonable straight line resulted when an inverse third power relationship was assumed (Figure 14). Thus, the cellulose-based mesophases examined to date show an inverse third power dependence of pitch on concentration. This is a markedly greater sensitivity of pitch to changes in concentration than that shown by polypeptide systems. Recently, Fried, Gilli, and Sixou[42] also found a solvent-dependent exponent greater than 3 for HPC in several organic solvents.

A higher concentration of cellulose-based chains is required to form a liquid crystalline phase[16,28,30] than is the case for the stiffer polypeptide chains.[43] Thus a cholesteric phase of a semiflexible polymer generally contains more polymer than an equivalent phase of a stiff-chain polymer. The exponent x in eq 10 for different systems does appear to be larger for more flexible polymers and therefore for higher polymer concentrations. In this context, the low exponent value of ~ 1.9 for the stiff carbohydrate schizophyllan[38] indicates that variations in x are not simply due to some intrinsic difference between carbohydrate-based and polypeptide-based systems.

Equation 10 is a purely empirical relationship. In a recent paper, Kimura and co-workers[22] presented a statistical theory for the ordering of an assembly of helical rodlike molecules. According to this theory, the cholesteric pitch is given as a function of temperature and concentration by

$$\frac{1}{P} = \frac{12}{\pi^2}\frac{\lambda\Delta}{LD}\phi f(\phi)\left(\frac{T_N}{T} - 1\right) \tag{11}$$

where

$$f(\phi) = [1 - (\phi/3)]/[1 - \phi]^2 \tag{12}$$

and ϕ is the bolume fraction of rods of length L and diameter D, λ and Δ are factors that characterize the helical shape of the molecules, T is the temperature of measurement, and T_N is the temperature at which the twist disappears ($P \rightarrow \infty$). Thus, for a given polymer, solvent, and temperature, the reciprocal pitch $1/P$ varies as $\phi f(\phi)$ and not as in eq 10 with a concentration-independent exponent, x.

The reciprocal pitch for three carbohydrate-based mesophases is plotted against $\phi f(\phi)$ in Figure 15. Curve 1, for a (hydroxypropyl)cellulose mesophase in water, was determined from our spectrophotometric measurements. Curve 2 was calculated from the results tabulated by Van et al.[38] for diffraction measurements on aqueous schizo-

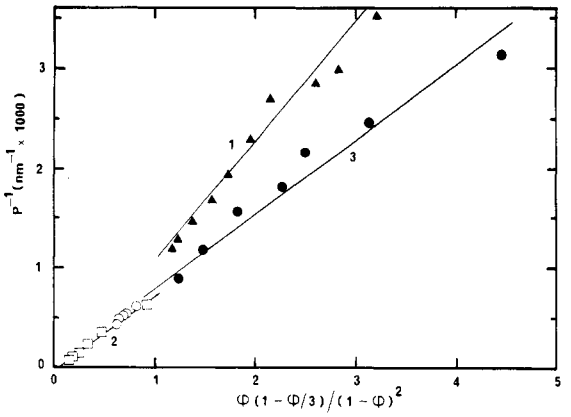

Figure 15. Plot of reciprocal pitch against $\phi(1 - \phi/3)/(1 - \phi)^2$: line 1 (triangles), spectrophotometric data for HPC-L in water; line 2 (squares), laser diffraction data for schizophyllan in water, calculated from data in ref 38; line 3, HPC-L in methanol (open circles are microscopic data, and closed circles are spectrophotometric data).

phyllan mesophases; the concentration is in weight rather than volume fractions, and a constant value for the refractive index was assumed. Curve 3 is the data for (hydroxypropyl)cellulose in methanol previously plotted in Figure 14. The data give reasonably linear plots that pass close to the origin. Thus, the concentration dependence of the cholesteric pitch is in fairly good agreement with the theory of Kimura et al.[22] Interpretation of the slope of the lines (Figure 15) in molecular terms requires quantitative measurements of pitch as a function of temperature and chain length.

The behavior of the currently known cellulosic cholesterics seems simpler than that of conventional cholesteryl esters and polypeptide-based systems. The ORD results reported here and in previous work[2,6,14,30] for a range of cellulosics and solvents are all compatible with a right-handed helicoidal arrangement.[44] Furthermore, the pitch for cellulose-based systems increases with increasing temperature.[3,6,7,16,45] Thus the reversal of handedness with solvent composition and temperature that has been observed for polypeptide[11] and low molar mass[46] cholesterics has not yet been observed for cellulosics. According to Kimura et al.[27] a thermally induced reversal should occur at temperatures above T_N (eq 11); T_N for the cellulose-based systems examined to date is apparently outside the accessible range of temperatures between the glass transition temperature and the clearing temperature. A solvent-induced reversal of cholesteric pitch is predicted to occur for a system of helical rods when the dielectric constant of the medium ϵ_m changes from $\epsilon_m \leq \bar{\epsilon}_c$ to $\epsilon_m \geq \bar{\epsilon}_c$, where $\bar{\epsilon}_c$ is the geometric mean of the two principal dielectric constants of the rod normal to the rod axis.[20] The right-handed twist for HPC mesophases indicates that if the molecules do in fact behave as helical rods (e.g., as the left-handed 3_2 helix proposed for crystalline HPC[23]), then the critical dielectric constant has not been attained. HPC has been examined in solvents ranging from water ($\epsilon = 80$) to dioxane ($\epsilon = 2.2$) without finding any evidence to date for reversal of twist.

Acknowledgment. Support from the Natural Sciences and Engineering Research Council of Canada (NSERC) and Hercules Inc. is gratefully acknowledged. R.S.W. thanks NSERC, the Quebec Government, and the Pulp and Paper Research Institute of Canada for scholarships. We are grateful to Mr. W. Q. Yean and Dr. S.-L. Tseng for providing assistance with the ultracentrifugation and spectrophotometry. We thank Professors Sixou, Uematsu, and Zugenmaier for preprints of their publications.

Registry No. HPC, 9004-64-2.

References and Notes

(1) D. G. Gray, *J. Appl. Polym. Sci., Appl. Polym. Symp.* **37**, 179 (1983) and references therein.
(2) R. S. Werbowyj and D. G. Gray, *Mol. Cryst. Liq. Cryst. Lett.*, **34**, 97 (1976).
(3) J. Maeno, FRG Patent Application 2704776 (1977); U.S. Patent 4132464 (1979).
(4) D. L. Patel and R. D. Gilbert, *J. Polym. Sci., Polym. Phys. Ed.*, **19**, 1499 (1981).
(5) S. N. Bhadani, and D. G. Gray, *Makromol. Chem., Rapid Commun.*, **3**, 449 (1982).
(6) S.-L. Tseng, A. Valente, and D. G. Gray, *Macromolecules*, **14**, 715 (1981).
(7) G. V. Laivins, S.-L. Tseng, and D. G. Gray, *Macromolecules*, **15**, 1262 (1982).
(8) S. Chandrasekhar, "Liquid Crystals", Cambridge University Press, London, 1977, Chapter 4.
(9) H. de Vries, *Acta Crystallogr.*, **4**, 219 (1951).
(10) C. Robinson, *Trans. Faraday Soc.*, **52**, 571 (1956).
(11) I. Uematsu and Y. Uematsu, to be published.
(12) "Klucel Hydroxypropyl Cellulose: Chemical and Physical Properties", Hercules Inc., Wilmington, DE, 1976.
(13) D.-S. Lee and A. S. Perlin, *Carbohydr. Res.*, **106**, 1 (1982).
(14) R. S. Werbowyj, Ph.D. Thesis, McGill University, Montreal, 1982.
(15) B. Nyström, and R. Bergman, *Eur. Polym. J.*, **14**, 431 (1978).
(16) R. S. Werbowyj and D. G. Gray, *Macromolecules*, **13**, 69 (1980).
(17) K. Kamide, T. Terakawa, and Y. Miyazaki, *Polym. J.*, **11**, 285 (1979).
(18) G. C. Berry and M. A. Leech in "Solution Properties of Polysaccharides", D. A. Brant, Ed., Washington, DC, 1981; ACS Symp. Ser. No. 150, p 61.
(19) P. Crabbé, "ORD and CD in Chemistry and Biochemistry", Academic Press, New York, 1972.
(20) T. V. Samulski and E. T. Samulski, *J. Chem. Phys.*, **67**, 824 (1977).
(21) A. Yu. Grosberg, *Sov. Phys. Dokl.*, **25**, 638 (1980).
(22) H. Kimura, M. Hosino, and H. Nakano, *J. Phys. Soc. Jpn.*, **51**, 1584 (1982).
(23) E. T. D. Atkins, W. S. Fulton, and M. J. Miles, Proceedings of the 5th International Dissolving Pulp Conference, Vienna, Tappi-Oezepa, 1980, p 208.
(24) M. Panar and L. F. Beste, *Polym. Prepr., Am. Chem. Soc., Div. Polym. Chem.*, **17**, 47 (1976).
(25) D. van Luyen, L. Liébert, and L. Strzelecki, *Eur. Polym. J.*, **16**, 307 (1980).
(26) K. H. Gardner and J. Blackwell, *Biopolymers*, **13**, 1975 (1974).
(27) H. Finkelmann and G. Rehage, *Makromol. Chem., Rapid Commun.*, **1**, 733 (1980).
(28) S. Dayan, P. Maissa, M. J. Vellutini, and P. Sixou, *J. Polym. Sci., Polym. Lett. Ed.*, **20**, 33 (1982).
(29) S. M. Aharoni, *Polym. Prepr., Am. Chem. Soc., Div. Polym. Chem.*, **22**, 116 (1981).
(30) S. N. Bhadani and D. G. Gray, *Makromol. Chem.*, **184**, 1727 (1983).
(31) J. L. Fergason, *Mol. Cryst. Liq. Cryst.*, **1**, 293 (1966).
(32) R. Dreker, G. Meier, and A. Saupe, *Mol. Cryst. Liq. Cryst.*, **13**, 17 (1971).
(33) C. Robinson, *Tetrahedron*, **13**, 219 (1961).
(34) G. Meenten and P. Navard, *Polymer*, **23**, 1727 (1982).
(35) G. W. Stroke in "Encyclopedia of Physics", Vol. 29, S. Flügge, Ed., Springer-Verlag, New York, 1967, p 457.
(36) T. Tsutsui and R. Tanaka, *Polym. J.*, **12**, 473 (1980).
(37) J. Bheda, J. F. Fellers, and J. L. White, *Colloid Polym. Sci.*, **258**, 1335 (1980).
(38) K. Van, T. Norisuye, and A. Teramoto, *Mol. Cryst. Liq. Cryst.*, **78**, 123 (1981).
(39) H. Toriumi, S. Minakuchi, and I. Uematsu, *J. Polym. Sci., Polym. Phys. Ed.*, **19**, 1167 (1981).
(40) E. Iizuka, *Polym. J.*, **10**, 293 (1978).
(41) Y. Onogi, J. L. White, and J. F. Fellers, *J. Polym. Sci., Polym. Phys. Ed.*, **18**, 663 (1980).
(42) F. Fried, J. M. Gilli, and P. Sixou, *Mol. Cryst. Liq. Cryst.*, **98**, 209 (1983).
(43) W. G. Miller, *Annu. Rev. Phys. Chem.*, **29**, 519 (1978).
(44) A recently discovered exception may be mentioned. Cellulose tricarbanilate in methyl ethyl ketone forms long-pitch cho-

lesteric liquid crystals whose pitch *decreases* with increasing solvent concentration and whose optical properties suggest a *left-handed* helicoidal arrangement. (U. Vogt and P. Zugenmaier, *Makromol. Chem., Rapid Commun.*, 4, 759 (1983)).

(45) I. Lematre, S. Dayan, and P. Sixou, *Mol. Cryst. Liq. Cryst.*, 84, 267 (1982).
(46) G. S. Chilaya and L. N. Lisetskii, *Sov. Phys. Usp.*, 24, 496 (1981).

Melting Point Depression in Crystalline/Compatible Polymer Blends

Peter B. Rim† and James P. Runt*

Department of Materials Science and Engineering, Polymer Science Program, The Pennsylvania State University, University Park, Pennsylvania 16802.
Received December 28, 1982

ABSTRACT: The determination of polymer/polymer interaction parameters (χ) from melting point data is critically reviewed with emphasis on two major areas. The first concerns variations of morphology with blend composition which can restrict attempts to calculate χ if nonequilibrium melting points are used. An equation is presented that relates the experimentally observed melting point change upon blending to the thermodynamic melting point depression and a morphological term that accounts for changes in lamellar thickness. Other morphological factors such as crystalline perfection and size are discussed. The second area of interest involves processes such as lamellar thickening during thermal analysis that can seriously impair determination of "true" crystalline melting points. Finally, methods for directly determining blend equilibrium melting points are discussed.

1. Introduction

In the past decade, blending or alloying polymers has been shown to be an excellent way of developing new materials exhibiting combinations of properties that cannot be obtained from any one polymer. Of special interest are those blends in which the component polymers are believed to be mixed on the molecular level. A large number of these "compatible" blends are composed of macromolecules that are chemically dissimilar. It is believed that specific interactions between unlike moieties are the driving force for miscibility in these systems. Chemically similar polymers can also exhibit compatibility. However, since the change in entropy upon mixing is small for two high molecular weight materials, the enthalpy of mixing cannot exceed a small critical value without phase separation occurring. It is for this reason that the rule of "like dissolves like" does not always apply to polymeric alloys.

There is a great deal of interest in compatible systems that contain at least one crystallizable component (crystalline/compatible blends). This is at least partially due to the fact that roughly one-half to two-thirds of all commercially significant polymers are crystalline or crystallizable. In these systems, the crystalline regions are phase separated from a miscible amorphous matrix.

Research on compatible blends, as well as polymer alloys in general, has expanded in the past 5–10 years as evidenced by the publication of a number of texts and review articles.[1-5] However, many questions remain unresolved. One of the most intriguing of these is the nature and extent of polymer/polymer compatibility. The most widely used technique for determining the magnitude of compatibility-inducing interactions in crystalline/compatible blends is melting point depression. The purpose of this article is to critically review this approach.

2. Background

Thermodynamic considerations predict that the chemical potential of a polymer will be decreased by the addition of a miscible diluent. If the polymer is crystallizable, this decrease in chemical potential will result in a decreased equilibrium melting point. Using the thermodynamic considerations of Scott,[6] Nishi and Wang[7] derived a relationship describing the melting point depression of a crystalline polymer due to the presence of a miscible diluent:

$$\frac{1}{T_m^{\circ\prime}} - \frac{1}{T_m^{\circ}} = \frac{-R\bar{V}_c}{\Delta H_f^{\circ}\bar{V}_a}\left[\frac{\ln V_c}{M_c} + \left(\frac{1}{M_c} - \frac{1}{M_a}\right)V_a\right] + \frac{-R\bar{V}_c}{\Delta H_f^{\circ}\bar{V}_a}(\chi V_a^2) \quad (1)$$

where $\bar{V}$ is the molar volume of the polymer repeat unit, V the volume fraction of the component in the blend, ΔH_f° the perfect crystal heat of fusion of the crystallizable polymer, M the degree of polymerization, R the universal gas constant, T_m° the equilibrium melting point of the pure crystallizable component, $T_m^{\circ\prime}$ the equilibrium melting point of the crystalline material in the blend, and χ the polymer/polymer interaction parameter. The subscripts a and c denote the amorphous and crystalline components, respectively. The first term on the right-hand side of eq 1 reflects the entropy of mixing contribution to the equilibrium melting point depression while the second term reflects the enthalpy of mixing contribution.

In the case where the miscible diluent is polymeric, the entropy of mixing becomes negligible and the melting point depression will be largely enthalpic in nature. Equation 1 then reduces to

$$\frac{1}{T_m^{\circ\prime}} - \frac{1}{T_m^{\circ}} = \frac{-R\bar{V}_c}{\Delta H_f^{\circ}\bar{V}_a}(\chi V_a^2) \quad (2)$$

The parameters of major interest in the preceding relationship are χ and V_a. Notice that for χ's less than zero, polymer/polymer interactions result in an equilibrium melting point depression. The smaller the value of χ, the greater the polymer/polymer interactions and the greater the melting point depression. Also note that $T_m^{\circ\prime}$ would

† Present address: Johnson Wax, Racine, WI 53403.

0024-9297/84/2217-1520$01.50/0